Computational Approach To Characterize Causative Factors and Molecular Indicators of Chronic Wound Inflammation

Sridevi Nagaraja, Anders Wallqvist, Jaques Reifman, and Alexander Y. Mitrophanov

Chronic inflammation is rapidly becoming recognized as a key contributor to numerous pathologies. Despite detailed investigations, understanding of the molecular mechanisms regulating inflammation is incomplete. Knowledge of such critical regulatory processes and informative indicators of chronic inflammation is necessary for efficacious therapeutic interventions and diagnostic support to clinicians. We used a computational modeling approach to elucidate the critical factors responsible for chronic inflammation and to identify robust molecular indicators of chronic inflammatory conditions. Our kinetic model successfully captured experimentally observed cell and cytokine dynamics for both acute and chronic inflammatory responses. Using sensitivity analysis, we identified macrophage influx and efflux rate modulation as the strongest inducing factor of chronic inflammation for a wide range of scenarios. Moreover, our model predicted that, among all major inflammatory mediators, IL-6, TGF-β, and PDGF may generally be considered the most sensitive and robust indicators of chronic inflammation, which is supported by existing, but limited, experimental evidence. ***The Journal of Immunology*****, 2014, 192: 1824–1834.**

Inflammation is an essential, nonspecific innate immune response that facilitates survival during infection, injury, and disease (1, 2). In the absence of a persistent initiator, a well-balanced inflammatory response usually resolves in ∼2 wk (3, 4). Inflammation is normally reduced when infiltrated leukocytes are eliminated from the inflamed site and the tissue populations of macrophages and lymphocytes return to their normal, preinflammation numbers and phenotypes (2, 3, 5). The inflammatory response is coordinated by a group of cell-derived molecular species known as cytokines, chemokines, and growth factors. Most cytokines are multifunctional and are involved in an extensive network that carries out positive and negative regulation of cell activation and behavior (6–8). Dysregulation of the inflammatory response may lead to prolonged arrest in an inflamed state, possibly resulting in host tissue damage and pathological chronic inflammation.

Chronic inflammation can be generally defined as a physiological state that is characterized by a prolonged and heightened inflammatory response (9, 10). It has been associated with various autoimmune, infectious, and neoplastic pathologies, including tumorigenesis, CNS disorders, diabetes, psoriasis, atherosclerosis, rheumatoid arthritis, asthma, and chronic wounds, among many others (2, 10, 11). Despite its central role in disease, the mechanistic details underlying the initiation and progression of chronic inflammation remain largely unresolved. In addition, reliable molecular indicators for the early detection of chronic inflammation have not been identified because of a lack of relevant data for human subjects. Chronic inflammatory pathologies have many manifestations, such as abnormal apoptotic neutrophil loading in diabetic ulcers (12) and increased presence of classically activated macrophages in chronic ischemic wounds (13). Yet, the most conspicuous and often-reported feature of many chronic (or delayed) inflammatory scenarios is the persistent presence of elevated levels of pro-inflammatory cytokines, such as TNF-α, IL-1β, and IL-6 (12, 14–17).

Animal model studies of chronic inflammation in wounds and diseases, such as obesity and atherosclerosis, have elucidated gene- and protein-level differences between normal and chronic inflammatory responses (12, 13). Yet, it has not been firmly established whether the expression of the same genes is altered in humans during disease, questioning the validity of such indicators. Any human study of chronic inflammatory diseases takes place well after the disease has already progressed and, thus, fails to provide insights into the factors triggering the chronic state (9, 18–22). Although chronic inflammation can be present in many pathological conditions, it is not causative to disease unless exacerbated by additional genetic and environmental factors (11). Therefore, attempts to alleviate chronic inflammation are confined to cases in which a disease has resulted, at which point the treatment is focused on addressing the symptoms of inflammation as opposed to its causative factors. As a result, many basic, mechanistic questions regarding the chronic state of the inflammatory process have remained unanswered.

Because of the inherent complexity of the inflammatory process and the aforementioned limitations of conventional approaches, these questions are difficult to answer via traditional experimentation alone. A complementary in silico approach has the unique advantage of providing focused and time-efficient integration and analysis of the available literature data, with the capability of generating experimentally testable hypotheses to expedite the investigative process. Although a number of mathematical models recently have been developed and applied to study inflammation

Department of Defense Biotechnology High-Performance Computing Software Applications Institute, Telemedicine and Advanced Technology Research Center, U.S. Army Medical Research and Materiel Command, Ft. Detrick, MD 21702

Received for publication September 18, 2013. Accepted for publication December 11, 2013.

This work was supported by the Clinical and Rehabilitative Medicine Research Program of the U.S. Army Medical Research and Materiel Command.

The opinions and assertions contained herein are private views of the authors and are not to be construed as official or as reflecting the views of the U.S. Army or the U.S. Department of Defense. This article has been approved for public release with unlimited distribution.

Address correspondence and reprint requests to Dr. Jaques Reifman, Department of Defense Biotechnology High-Performance Computing Software Applications Institute, Telemedicine and Advanced Technology Research Center, U.S. Army Medical Research and Materiel Command, ATTN: MCMR-TT, 504 Scott Street, Ft. Detrick, MD 21702. E-mail address: jaques.reifman.civ@mail.mil

The online version of this article contains supplemental material.

Abbreviation used in this article: DDE, delay differential equation.

www.jimmunol.org/cgi/doi/10.4049/jimmunol.1302481

(23–33), their limited scope and focus predominantly on qualitative representations of inflammation dynamics generally restrict their ability to provide accurate interpretations of existing data sets and generate (semi)quantitative hypotheses. In this article, we introduce a kinetic, inherently quantitative computational model of inflammation whose parameters were derived directly from in vitro data. We validated the model using experimental data on acute inflammation and then extended it to investigate chronic inflammatory scenarios.

Our modeling results suggest that the modulation of two mechanistic parameters, macrophage influx and efflux rates, may be the strongest general trigger of chronic inflammation. Moreover, we predicted that local concentration changes of three molecular mediators—IL-6, TGF-β, and PDGF—may be sensitive and robust indicators of the ongoing or imminent chronic inflammatory response under various scenarios. Our results are in agreement with existing experimental and clinical data and suggest that key dynamic features of the inflammatory response can be explained and predicted using a parsimonious computational modeling approach.

Materials and Methods

Computational model and simulations

Our mathematical model represents local inflammation in a wound. The model consists of 15 ordinary differential equations and 1 delay differential equation (DDE; Table I), and it has 69 main parameters representing different molecular and cellular processes, such as neutrophil and macrophage phenotype conversion, phagocytosis of apoptotic neutrophils, and the production and degradation of cytokines and growth factors (Supplemental Table I; note that the 19 chemotaxis function parameters in the model are regarded as a separate group and are not included among the main parameters). In the model, we included the cell types, cytokines, and growth factors that are commonly regarded as key components of the inflammatory response (Fig. 1). The DDE in the model is used to describe pro-inflammatory macrophage dynamics. In the bloodstream, macrophages exist in the form of their precursors (i.e., monocytes), which migrate at rates similar to those for neutrophil migration (34) and then differentiate into active macrophages at the site of inflammation within ∼12−48 h (16). Because we did not explicitly define monocyte kinetics in our model, we represented monocyte differentiation by incorporating a 12-h delay in the argument of the chemotaxis function that drives pro-inflammatory macrophage migration in the model (33) (Table I).

The time courses for the concentrations of these cell types and molecular species constitute the output of our model. Its main input is the initial platelet concentration (default value: 2×10^8 platelets/ml), which represents an injury initiating local inflammation (all other model variables are initially set to 0). The model equations were solved numerically using the MATLAB solver DDE23 with default tolerance values. Our model is intrinsically quantitative, because all of its variables and main parameters (except the dimensionless feedback functions discussed below) are expressed in absolute units, and the majority of the parameter values were derived directly from experimental data. We performed all computations in MATLAB 2012a (MathWorks, Natick, MA). Each simulation covered a 20-d time interval after inflammation initiation.

In the model, we assume that the inflammatory response is initiated only by TGF-β released by platelets postinjury. Although the inflammatory response also can be stimulated by other locally secreted chemoattractants [such as PDGF, TNF-α, MIP-1α, and CXCL8 (35–37)], TGF-β has been characterized as the strongest inflammatory cell chemoattractant in vitro (38, 39) and is used in our model as a proxy for all initiating chemotactic signals. In the model, we assume that anti-inflammatory macrophages are generated by phenotype conversion of pro-inflammatory macrophages triggered by phagocytosis of apoptotic neutrophils, which is suggested by experimental data (40–42). Yet another modeling assumption pertains to the activity of TGF-β and IL-1β. When released from various cellular sources, TGF-β exists in a latent state (43) and is subsequently activated by the presence of injury- and infection-related enzymes, as well as the acidic and elevated-temperature environment of the inflamed site (44). Analogously, the biological activity of IL-1β requires its maturation into an activated form, which occurs during or after secretion through the cell membrane and is preceded by inflammasome-mediated cleavage of the translated IL-1β (45, 46). We do not explicitly define the kinetics of TGF-β or IL-1β activation and use the simplifying assumption that, because inflammation is present, any latent TGF-β or IL-1β that is released will be in its activated form.

Estimation of production rates

Among its 69 main parameters, our computational model contains 26 production rates. Using published data from in vitro experiments, the production rates were estimated as follows:

$$k = \frac{C}{Mt} \tag{1}$$

where k is the production rate for a cytokine or growth factor, C is the concentration of the cytokine (growth factor) measured in the supernatant from the cell culture after incubation, M is the initial concentration of macrophage suspension in the cell culture experiment, and t is the time of incubation of macrophages with a stimulant (e.g., bacterial load or endotoxin). In cases where measurements were available for multiple time points, linear regression was used to calculate slopes, which were subsequently divided by the initial macrophage concentration to give the final production rate values. As an illustration, Fig. 2A and 2B show the IL-1β, TNF-α, and IL-10 production rate estimation for pro- and anti-inflammatory macrophages. To approximate the chemotactic migration data for neutrophils and monocytes (38, 39), we used a combination of quadratic and linear functions with at least three parameters (Fig. 2C, 2D).

Estimation of degradation rates

The model contains 12 degradation/removal rates. Half-life estimates for the catabolic breakdown of cytokines and growth factors were obtained from the literature. Assuming a first-order decay of the molecular species, the degradation rates were calculated as follows:

$$k = \frac{0.693}{t_{1/2}} \tag{2}$$

where $t_{1/2}$ is the half-life of a cytokine or growth factor, and k is the corresponding degradation rate.

Estimation of the parameters describing phagocytosis of apoptotic neutrophils by pro-inflammatory macrophages

Pro-inflammatory macrophages undergo a change in phenotype upon phagocytizing apoptotic neutrophils and cellular debris (40–42). In our model, the phagocytosis rate of apoptotic neutrophils and phenotype conversion rate for macrophages were determined by approximating experimental phagocytosis data using hyperbolic functions. For example, the data by Newman et al. (47) characterize the number of apoptotic neutrophils ingested after 4 h of incubation with a fixed initial concentration of macrophages for different initial concentrations of apoptotic neutrophils. These data were converted into rates of apoptotic neutrophil ingestion per pro-inflammatory macrophage per hour for different initial apoptotic neutrophil concentrations (Supplemental Fig. 1A) and were then fitted with the following equation:

$$g(N_{apop}) = \frac{k_{1ingest} N_{apop}}{k_{2ingest} + N_{apop}} \tag{3}$$

where N_{apop} is the concentration of apoptotic neutrophils, and $k_{1ingest}$ and $k_{2ingest}$ are the model parameters that were estimated as a result of the fitting (Supplemental Table I). The fitting was performed using MATLAB's curve-fitting toolbox.

An expression similar to Eq. 3 was used to describe the rate of phenotype conversion of pro-inflammatory into anti-inflammatory macrophages, which occurs as a result of apoptotic neutrophil phagocytosis by pro-inflammatory macrophages. However, phagocytosis is not a "one-on-one process" (i.e., a single macrophage can phagocytize up to three apoptotic neutrophils) (41, 48, 49). Using the data reported by Newman et al. (47), we calculated the fraction of macrophages ingesting apoptotic neutrophils per hour for different initial concentrations of apoptotic neutrophils (Supplemental Fig. 1B). These data were then fitted with the following equation:

$$\tilde{g}(N_{apop}) = \frac{\tilde{k}_{1ingest} N_{apop}}{\tilde{k}_{2ingest} + N_{apop}} \tag{4}$$

where $\tilde{k}_{1ingest}$ and $\tilde{k}_{2ingest}$ are the model parameters that were estimated as a result of the fitting (Supplemental Table I).

Estimation of cytokine feedback functions

Pro- and anti-inflammatory macrophages, neutrophils, and platelets secrete cytokines and growth factors that provide regulatory feedback for the inflammatory response by upregulating (positive feedback) or downregulating (negative feedback) the production of other cytokines. (We generally regard these interactions as feedbacks because they represent the self-modulating effects of extracellular mediators on the intracellular machinery responsible for the production of such mediators.) To reflect these effects in the model, we introduced 10 dimensionless feedback functions denoted $f_1, f_2, \ldots, f_{10}$ (Supplemental Table I) that represent fractional increases or decreases (induced by a particular cytokine or growth factor) in the production rates of other cytokines and growth factors for pro-inflammatory macrophages. The parameters of these functions were estimated by fitting the functions to experimental data using the curve-fitting toolbox in MATLAB (Supplemental Fig. 1C).

Sensitivity analysis

We calculated logarithmic (i.e., relative) local sensitivities, $s_{ij}(t)$, at time moments t, according to the standard definition (see, e.g., Ref. 50):

$$s_{ij}(t) = \partial \log X_i(t) / \partial \log p_j = (\mathrm{d}X_i/X_i)/(\mathrm{d}p_j/p_j) \quad (5)$$

where $X_i(t)$ is the model's ith variable and p_j is the model's jth parameter (of the model's 69 main parameters). By definition, each of these sensitivities reflects the magnitude of the relative change in a model's output variable induced by a local (i.e., small) relative change in a model's parameter. To obtain numeric approximations of the derivatives in Eq. 5, each parameter was individually perturbed by $\pm 1\%$ of its value, and the derivative was approximated using the second-order central finite difference formula. We performed local sensitivity analysis in the vicinity of the default parameter set, as well as for 10,000 random parameter sets in which individual parameters were sampled independently from intervals, permitting up to 2-fold deviations (up or down) from the corresponding default values. This random sampling was intended to represent possible natural variations in the molecular environment of the inflamed site for different subjects under different inflammatory scenarios. To generate the random parameter sets, we used Latin hypercube sampling, as previously described (51) (we used the MATLAB function LHSDESIGN). In all analyses, we calculated local sensitivities for each of the 21 evenly spaced time points that discretize the total 20-d simulation interval into 1-d subintervals (i.e., day 0, day 1, and so forth). To compare and rank sensitivities, we used their absolute values.

Results

Model captures essential kinetic features of acute inflammation

We tested our model's ability to capture typical features of the time course of acute inflammation by comparing modeling predictions with published experimental data. The model includes descriptions for key mechanisms involved in the inflammatory response (Fig. 1), with the parameters quantifying these mechanisms derived from acute inflammatory response data (Fig. 2). The model predicted the occurrence of a neutrophil peak at ~1 d and a macrophage peak at ~2 d after inflammation initiation (Fig. 3A, 3B). These predictions are in accord with experimental measurements showing that a single, well-pronounced peak typically occurs at 1−3 d after inflammation initiation for neutrophils and at 2−4 d for macrophages (3, 52). Furthermore, it is expected that the concentrations of the inflammatory cells and cytokines return to their basal level within 2−3 wk after the onset of inflammation (3, 4, 52). Our model predicted the return of all variables in the model to their default values within 20 d after inflammation initiation (Fig. 3A–3C). Moreover, our model predicted the kinetics of individual neutrophil and macrophage phenotypes (Supplemental Fig. 2).

To further validate our computational model, we compared its predictions with the dynamics of acute inflammatory response in a number of animal and human in vivo models (those datasets were not used to estimate the model parameters). The computational model successfully predicted key features (such as the overall curve shape, peak time, and resolution time) for neutrophil and macrophage time courses, as observed in human wounds (52), and for peritoneal infection in mice (16) (Fig. 3A, 3B). We validated TGF-β concentration predictions using experimental data from rats with excisional wound injury (53) (Fig. 3C). Most of the cytokines and chemokines in our model showed good qualitative or semiquantitative agreement with available inflammation data. As an illustration, we show modeling predictions and their experimental validation (with experimental data taken from Ref. 54) for two representative cytokines with pro-inflammatory (IL-1β) and anti-inflammatory (IL-10) properties in Fig. 3D and 3E. Interestingly, for two of the cytokines [IL-12 (Fig. 3F) and IL-6 (data not shown)], our model gave quantitatively accurate kinetic predictions. Opportunities for a more extensive quantitative validation were limited as the result of interassay and interlaboratory variations in the measured concentrations of inflammatory cells and molecular mediators.

Modeling predicts macrophage influx and efflux modulation to be the strongest mechanistic trigger of chronic inflammation

Our analysis of chronic inflammation was based on the general assumption that delayed resolution of inflammation results from dysregulation of certain key mechanisms that are represented by the main parameters in our model. We used this assumption to extend our acute inflammation model to represent chronic inflammatory scenarios. This was achieved by performing an extensive sensitivity analysis to identify the parameters that may display a strong functional association with chronic inflammation.

Experimental data suggest that the pro-inflammatory cytokines TNF-α, IL-1β, and IL-6 are consistently and considerably increased in chronic inflammation induced by infection or disease, such as diabetes (12, 14–17). We initially used local sensitivity analysis in the vicinity of the default parameter set (see *Materials and Methods*) to identify the parameters whose change induced the largest variation in the concentrations of TNF-α, IL-1β, and IL-6 (analyzed independently). We found that, for each of the three cytokines, the largest relative changes (for the majority of the time points considered in the sensitivity analysis) were induced by modulating the same two parameters of the total 69 main parameters. These two parameters represented the pro-inflammatory macrophage influx rate and the rate of efflux of both pro- and anti-inflammatory macrophages (designated as k_{M_in} and k_{d_M} in the model, respectively; Table I, Supplemental Table I). For earlier time points in the simulation (~2–10 d after inflammation initiation), macrophage influx rate had the highest impact on the cytokine concentrations (Fig. 4A), whereas macrophage efflux rate had the second highest influence on those outputs (data not shown). At later time points (~7–20 d after inflammation initiation), the macrophage efflux rate emerged as the strongest modulator of the levels of all three cytokines (Fig. 4A), and the macrophage influx rate was the second strongest (data not shown). Overall, these two parameters represented the dominant factors leading to the overproduction of TNF-α, IL-1β, and IL-6 in our model.

We tested the robustness of these results by performing local sensitivity analysis in the vicinities of 10,000 randomly selected parameter sets. Specifically, we identified the parameters that induced the largest variations in the concentrations of the three cytokines (i.e., TNF-α, IL-1β, and IL-6) across 10,000 simulations with random parameter sets (see *Materials and Methods*). We verified that, for >70% of the simulations, the sensitivities for the two parameters (i.e., macrophage influx and efflux rates) were the highest for the majority of the considered simulation time points. (Specifically, the macrophage influx rate was the most sensitive parameter at days 4−9 after inflammation initiation for TNF-α; at

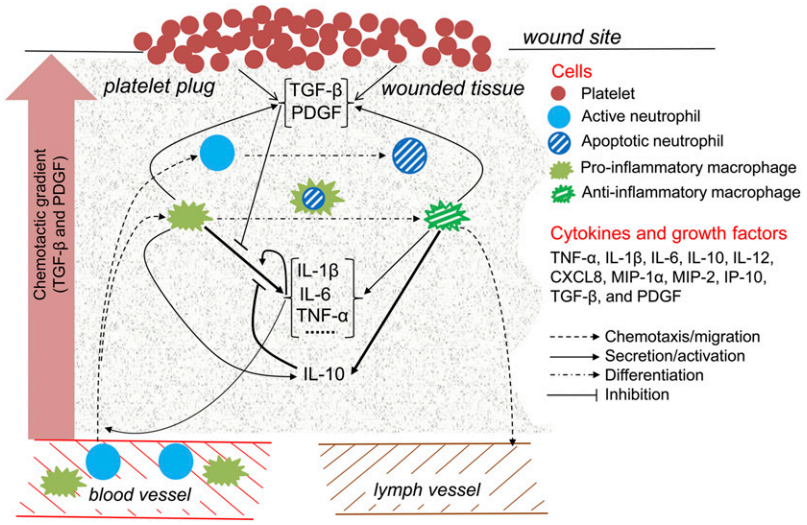

FIGURE 1. Inflammation model components and interactions. Platelets initiate the wound-healing process by supporting blood clotting in the wound. They also secrete growth factors, such as TGF-β and PDGF, which promote the migration of neutrophils and monocytes from surrounding blood vessels (43, 86). Monocytes mature into pro-inflammatory macrophages at the wound site. Neutrophils ingest cellular debris and the invading bacteria and, as a result, become apoptotic (1). Pro-inflammatory macrophages then phagocytize the apoptotic neutrophils (and cellular debris) and change their phenotype to anti-inflammatory (41). Both pro- and anti-inflammatory macrophages secrete cytokines and growth factors at different rates, and these molecular mediators provide positive and/or negative feedback to the ongoing inflammation (6, 87). Anti-inflammatory macrophages are cleared by migration to lymphatic vessels (88).

days 2, 6, and 7 for IL-1β; and at days 2−10 for IL-6. The macrophage efflux rate was the most sensitive parameter at days 10−20 after inflammation initiation for TNF-α; at days 8−20 for IL-1β; and at days 11−20 for IL-6.) Representative simulation results for 3 d (days 4, 10, and 16) are shown in Fig. 4B. For each of the 10,000 randomly selected parameter sets, just like for the default parameter set, macrophage influx rate had the largest influence on all three cytokines at earlier simulation time points, whereas macrophage efflux rate dominated at later times. This result is consistent with the dominant role of macrophage influx during inflammation initiation and the prevalent role of macrophage efflux from the inflamed site during inflammation resolution. Notably, the two parameters induced changes in opposite directions: an increase in the concentrations of the three cytokines could be caused by increasing macrophage influx rate or by decreasing macrophage efflux rate. Taken together, our results suggest that macrophage flux modulation may be a principal cause of a delay in inflammation resolution. This general prediction is consistent with studies showing that a decrease in macrophage efflux from the wound, resulting from disrupted synthesis of the integrin Mac-1, delayed wound healing in mice (55, 56).

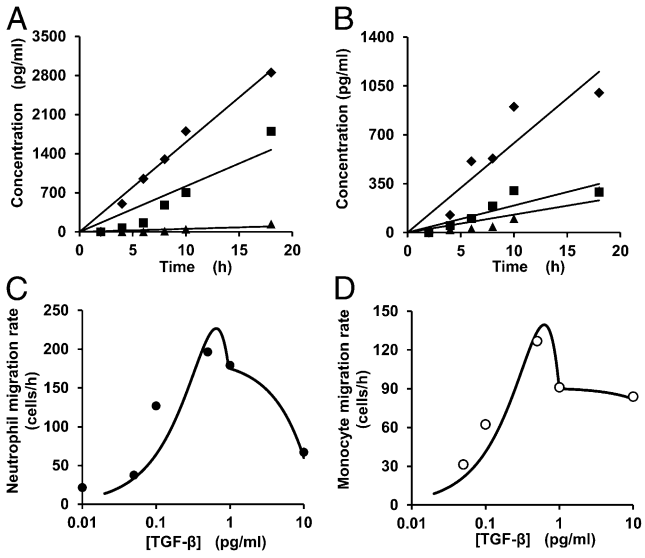

FIGURE 2. Estimation of cytokine production rates and chemotaxis functions from experimental data. Experimental data on the production of IL-1β (♦), TNF-α (■), and IL-10 (▲) were obtained for cultured human pro-inflammatory (**A**) and anti-inflammatory (**B**) monocytes (40) and approximated using linear regression analysis (solid lines). The slopes of the regression lines represent estimated cytokine production rates. Experimental data on neutrophil (●; **C**) and monocyte (○; **D**) chemotaxis induced by TGF-β were obtained from Brandes et al. (39) and Wahl et al. (38). The migration rate functions for both neutrophils and monocytes were obtained by fitting the experimental data using a combination of quadratic and linear functions (solid lines).

Our local sensitivity analysis results suggested that comparatively large changes in macrophage influx and efflux rates can induce a considerable and possibly sustained increase in the levels of inflammatory cells, which may be indicative of chronic inflammation. We tested this prediction by increasing the default value of macrophage influx rate by 5-fold, which led to a noticeable increase in the total neutrophil concentration and a considerable increase in the total macrophage concentration (Fig. 5). In comparison with an acute inflammatory scenario, macrophage resolution was delayed significantly, as is expected for chronic inflammation. We validated these computational predictions by comparisons with experimental data from an in vivo mouse model for both acute and delayed inflammatory response induced by the endotoxin zymosan given i.p. (16) (Fig. 5). [Such a comparison was justified by the assumption that a higher dose of endotoxin administration leads to an increased macrophage influx into the inflamed area (14, 57)]. In summary, these results demonstrate that the processes of macrophage influx and efflux may be critical to a well-balanced inflammatory response and that their dysregulation is a strong trigger of chronic inflammation.

Modeling identifies IL-6, TGF-β, and PDGF as sensitive local indicators of chronic inflammation

Having established that macrophage influx and efflux rates may play a defining role in the genesis of chronic inflammation, we wanted to determine which of the 11 model variables representing inflammatory mediators would be most sensitive to the modulation of macrophage flux rates. We first analyzed the logarithmic sensitivities for these 11 variables (one at a time) with respect to the two parameters (i.e., macrophage influx and efflux rates) for the default parameter set. This analysis showed that, at each of the considered simulation time points with the exception of day 1 after inflammation initiation, the concentrations of IL-6, TGF-β, and PDGF were characterized by the highest, second-highest, and third-highest sensitivities, respectively, for both of the perturbed macrophage flux parameters. This finding suggested that these three variables could be sensitive indicators of chronic inflammatory conditions induced by variations in the macrophage flux rates.

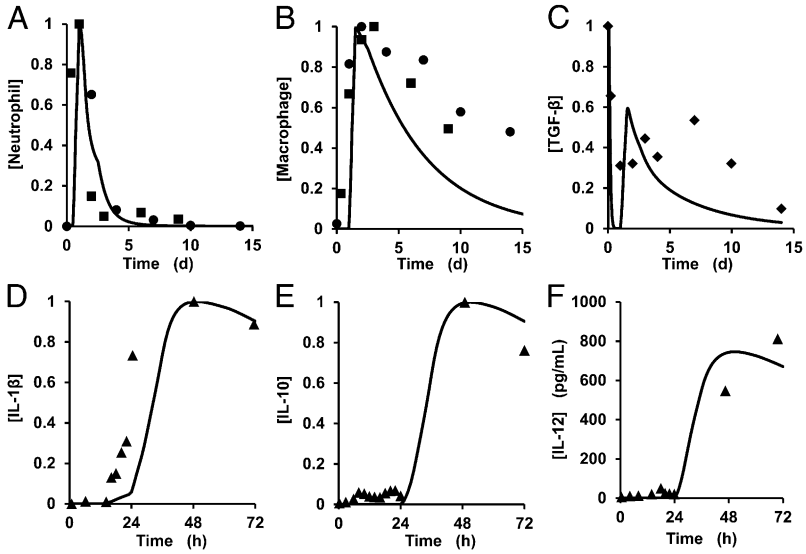

FIGURE 3. Modeling predictions capture experimentally detected kinetics of acute inflammation. Solid lines show modeling predictions; symbols show experimental data. Brackets designate concentration. (**A**–**C**) Experimental data for mouse infection (■) (16), rat wounds (♦) (53), and human wounds (●) (52). (**D** and **E**) Normalized values of IL-1β and IL-10 concentrations in vitro. Experimental data from cultured human macrophages are shown (▲) (54). For proper comparisons between model predictions and experimental data, normalization was necessary because of differences in reporting units between experimental data and model outputs and was achieved by division of all of the predicted or experimentally obtained values of a particular variable by the maximum value of that variable. (**F**) IL-12 concentration dynamics in vitro. Experimental data were taken from Kum et al. (54).

To test the robustness of these indicators, we analyzed the logarithmic sensitivities for the 10,000 randomly selected parameter sets. For each of the considered 21 simulation time points and each of the 11 variables, we calculated the fractions of the random parameter sets for which a given variable demonstrated the highest, second-highest, or third-highest sensitivity with respect to macrophage influx or efflux rate perturbations. Figs. 6 and 7 show the results for 4 d in the simulation (days 2, 4, 10, and 16 after inflammation initiation). These fractions were then averaged over the first 10 d after inflammation initiation, because we focused on the clinically important, early phases of inflammation development. We found that IL-6 concentration ranked as the most sensitive variable for an average of 84% of the randomly selected parameter sets when the perturbed parameter was macrophage influx rate and for an average of 67% of the randomly selected parameter sets when the perturbed parameter was macrophage efflux rate. TGF-β concentration ranked as the second most sensitive variable for 66 and 61% (on the average) of the parameter sets when the perturbed parameters were macrophage influx rate and macrophage efflux rate, respectively. Likewise, for these two flux parameters, PDGF concentration ranked as the third most sensitive variable for 68 and 50% of the parameter sets, respectively.

These results demonstrate that, among all of the inflammatory mediators represented in the model, IL-6, TGF-β, and PDGF had the largest relative changes induced by chronic inflammation triggers. Although the levels of TNF-α and IL-1β [often reported in the literature as chronic inflammation indicators (12, 14–17)] also can be increased by macrophage flux modulation, the relative magnitude of those increases in our modeling predictions appeared to be generally smaller than those for IL-6, TGF-β, and PDGF. Our findings suggest that these three molecular mediators (particularly IL-6) can be used as reliable early indicators of chronic inflammation in clinical settings. Interestingly, this conclusion is consistent with a recent clinical study of combat wounds by Hawksworth et al. (19), which identified local IL-6 level as the best predictor of dehiscence in traumatic wounds.

Model robustness analysis

We verified the robustness of the constructed computational model in the vicinity of the default parameter set using local sensitivity analysis, as described in *Materials and Methods*. Specifically, we confirmed that none of the model's 16 output variables was overly sensitive [i.e., $s_{ij}(t) > 10$] to any of the parameter perturbations. Because a major source of complexity in the inflammatory system is the functional (feedback) interactions between different inflammatory mediators, we chose to limit such feedbacks represented in the model (Supplemental Table I) to only those whose elimination (modeled by setting the corresponding feedback functions to 1) significantly (i.e., by ≥5%) affected at least one of the model outputs. One such feedback, present in an earlier version of the model, represented the downregulation of the production of the pro-inflammatory chemokine CXCL8 by the anti-inflammatory cytokine IL-10. This functional connection did not meet the above selection criterion and was excluded from the current version of the model. Interestingly, all of the major results reported in the preceding subsections for the current version of the model also held for the version in which that feedback interaction was present.

We found that elimination of a single feedback induced a ≥5% change only in the variable that the feedback directly modulated (i.e., its "affected" variable; see Supplemental Table I). However, it is conceivable that eliminating all feedbacks associated with one or more "effector" variables (i.e., the independent variable of the corresponding feedback functions; see Supplemental Table I) could considerably influence other variables in addition to the feedbacks' "affected" variables. To investigate this possibility, we performed simulations in which we simultaneously eliminated all feedbacks driven by the anti-inflammatory mediators TGF-β and IL-10 (feedback functions f_4, f_5, f_9, f_{10} and f_1, f_2, f_3, respectively; see Supplemental Table I) for the acute and chronic inflammatory scenarios. Indeed, elimination of these two groups of feedbacks induced a ≥5% change in the neutrophil and macrophage concentrations for both acute and chronic inflammation (Supplemental Fig. 3C, 3D), demonstrating the importance of interactions among feedbacks. The resulting changes for chronic inflammation were comparatively large (up to ~50 and ~100% for neutrophils and macrophages, respectively; compare dashed and dash-dotted lines in Supplemental Fig. 3C, 3D) and exceeded those for acute inflammation. This indicates that functional contributions of feedbacks can have increased significance when the inflammatory process is pathologically perturbed.

To investigate the effects of feedback control exerted by pro-inflammatory mediators, we performed a simulation in which TNF-α (and therefore all of the associated feedbacks) was "knocked out" (which was modeled by setting all of the TNF-α

Table I. Model variables and equations

Model variables: volume concentrations for different cell types and molecular species			
N_{act}	Active neutrophils	$TGF\beta$	Transforming growth factor-β
N_{apop}	Apoptotic neutrophils	$PDGF$	Platelet-derived growth factor
M_{pro}	Pro-inflammatory macrophages	$IL1\beta$	Interleukin-1β
M_{anti}	Anti-inflammatory macrophages	$IL6$	Interleukin-6
P	Platelets	$MIP1\alpha$	Macrophage inflammatory protein-1α
$CXCL8$	Chemokine $CXCL8$	$MIP2$	Macrophage inflammatory protein-2
$IL12$	Interleukin-12	$IP10$	Interferon-γ-induced protein 10
$IL10$	Interleukin-10	$TNF\alpha$	Tumor necrosis factor-α

Model equations

$$dP/dt = -k_{d\_P}P;$$

$$dN_{act}/dt = k_{N\_in}\{f_N(TGF\beta) + f_N(PDGF) + f(CXCL8)\} - k_{N\_deact}N_{act};$$

$$dN_{apopt}/dt = k_{N\_deact}N_{act} - \frac{k_{1ingest}N_{apop}}{k_{2ingest} + N_{apop}}M_{pro};$$

$$dM_{pro}/dt = k_{M\_in}\{f_M(TGF\beta(t-12)) + f_M(PDGF) + f(TNF\alpha) + f(MIP1\alpha)\}$$
$$-\left(\frac{\tilde{k}_{1ingest}N_{apop}}{\tilde{k}_{2ingest} + N_{apop}}\right)M_{pro} - k_{d\_M}\left(1 - 4\frac{\tilde{k}_{1ingest}N_{apop}}{\tilde{k}_{2ingest} + N_{apop}}\right)M_{pro};$$

$$dM_{anti}/dt = ((\tilde{k}_{1ingest}N_{apop})/(\tilde{k}_{2ingest} + N_{apop}))M_{pro} - k_{d\_M}M_{anti};$$

$$dTNF\alpha/dt = k_{TNF\alpha\_act}N_{act} + k_{TNF\alpha\_pro}f_1f_4f_6M_{pro} + k_{TNF\alpha\_anti}M_{anti} - k_{d\_TNF\alpha}TNF\alpha;$$

$$dTGF\beta/dt = k_{T\_P}P + k_{TGF\beta\_pro}M_{pro} + k_{TGF\beta\_anti}M_{anti} - k_{d\_TGF\beta}TGF\beta;$$

$$dPDGF/dt = k_{PDGF\_pro}M_{pro} + k_{PDGF\_anti}M_{anti} - k_{d\_PDGF}PDGF;$$

$$dIL1\beta/dt = k_{IL1\beta\_act}N_{act} + k_{IL1\beta\_pro}f_3f_5f_7M_{pro} + k_{IL1\beta\_anti}M_{anti} - k_{d\_IL1\beta}IL1\beta;$$

$$dCXCL8/dt = k_{CXCL8\_pro}M_{pro} + k_{CXCL8\_anti}M_{anti} - k_{d\_CXCL8}CXCL8;$$

$$dIL6/dt = k_{IL6\_act}N_{act} + k_{IL6\_pro}f_2(1+f_9)M_{pro} + k_{IL6\_anti}M_{anti} - k_{d\_IL6}IL6;$$

$$dIL10/dt = k_{IL10\_pro}(1+f_{10})M_{pro} + k_{IL10\_anti}M_{anti} - k_{d\_IL10}IL10;$$

$$dIL12/dt = k_{IL12\_pro}f_8M_{pro} - k_{d\_IL12}IL12;$$

$$dMIP1\alpha/dt = k_{MIP1\alpha\_pro}M_{pro} + k_{MIP1\alpha\_anti}M_{anti} - k_{d\_MIP1\alpha}MIP1\alpha;$$

$$dMIP2/dt = k_{MIP2\_pro}M_{pro} + k_{MIP2\_anti}M_{anti} - k_{d\_MIP2}MIP2;$$

$$dIP10/dt = k_{IP10\_pro}M_{pro} + k_{IP10\_anti}M_{anti} - k_{d\_IP10}IP10.$$

All cell concentration variables in our model are expressed in units of cells/ml. Variables for molecular mediators (cytokines, chemokines, and growth factors) are expressed in units of ng/ml. Time is expressed in hours. Feedback and chemotaxis functions for different cytokines were numbered and are described in detail in Supplemental Table I.

production rates to 0). The simulated TNF-α knockout resulted in decreased concentration peaks for neutrophils and macrophages, which is consistent with the experimentally observed decrease in the leukocyte levels in the wounds of the TNF-α receptor p55–knockout mice (58) (Supplemental Fig. 3A, 3B). Taken together, our findings support the notion that feedback regulation is important for fine-tuning the inflammatory response.

The first working version of our model comprised only 11 variables and 28 parameters and was much simpler than the current version (which is discussed in this article). It did not contain the positive- and negative-feedback interactions between the cytokines shown in Supplemental Table I. Moreover, it described the chemotactic effects of only two (TGF-β and PDGF) of the five (TGF-β, PDGF, CXCL8, TNF-α, and MIP-1α) molecular mediators whose chemotactic effects are reflected in the current version of the model. Yet, perhaps surprisingly, even that simpler model gave kinetic predictions that were in good agreement with experimentally detected acute inflammatory behavior (data not shown). This finding suggests that, although the current version of the model is a simplified representation of the complexity of the inflammatory process in vivo, our omission of many of its functional details did not seem to have precluded the generation of reasonable predictions. Furthermore, local sensitivity analysis of our original model predicted the same two mechanisms crucial for triggering chronic inflammation as the more comprehensive, current version of the model. The most sensitive indicator of chronic inflammation predicted by the original, simpler model was IL-6, whereas TNF-α and TGF-β appeared among the three most sensitive indicators. These results suggest that key properties of the inflammatory process might be largely insensitive to the details of many complex interactions occurring in the system and can be understood by considering only the essential molecular and cellular mechanisms.

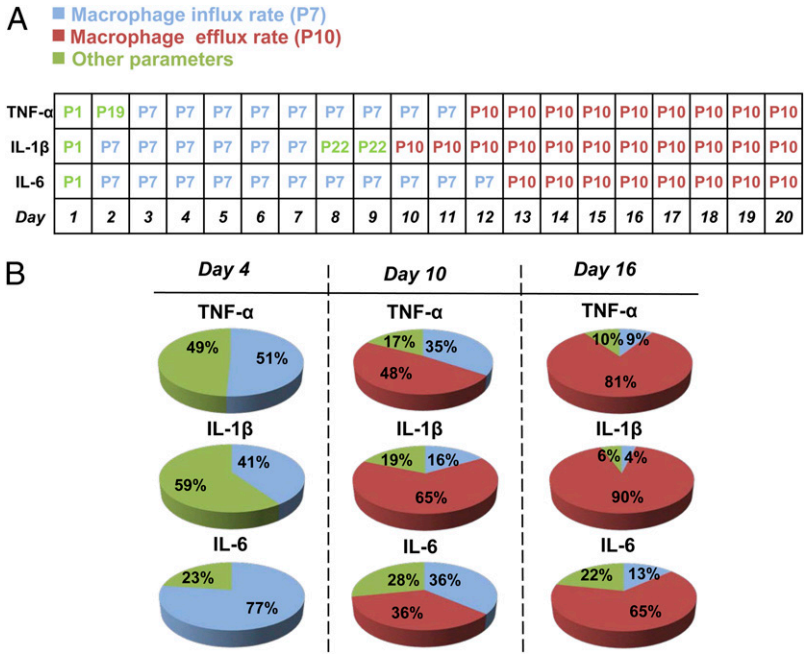

FIGURE 4. Sensitivity analysis identifies strong triggers of chronic inflammation. (**A**) Parameters inducing the largest changes in TNF-α, IL-1β, and IL-6 concentrations identified by local sensitivity analysis in the vicinity of the default parameter set (see *Materials and Methods*). (**B**) Summary of local sensitivity analysis results for 10,000 randomly selected parameter sets (see *Materials and Methods*) for three representative days (4, 10, and 16). Shown is the percentage of the 10,000 simulations for which the macrophage influx (blue) and efflux (red) parameters [identified in the analysis in (A)] induced the largest changes in TNF-α, IL-1β, and IL-6.

Discussion

Chronic inflammation is becoming increasingly recognized as a major contributor to several known pathologies, such as cancer, rheumatoid arthritis, and diabetic ulcers, among many others (10, 11). Yet, mechanistic causative factors of chronic inflammation, as well as its reliable molecular indicators, have not been sufficiently characterized. In this study, we used computational modeling approaches to gain mechanistic insights into chronic inflammation. Our differential equation–based model successfully predicted key kinetic features of the local acute and chronic inflammatory response, as was verified by direct comparisons of modeling predictions with experimental data. Using sensitivity analysis, we predicted that the levels of the pro-inflammatory cytokines IL-6, IL-1β, and TNF-α are affected the most by the same two model parameters: the rates of macrophage influx into and efflux out of the inflamed site. Because the levels of these cytokines are typically elevated in chronic inflammation, our results suggest that the two macrophage flux parameters may represent the mechanisms whose malfunction often delays normal resolution of inflammation. Furthermore, using our computational model, we established that different model variables respond differently to macrophage flux modulation. Of the 11 model variables representing inflammatory mediators, the concentrations of IL-6, TGF-β, and PDGF (in order of decreasing effect magnitude) were most affected by macrophage influx and efflux rate modulation. This finding indicates the possibility of using these three proteins, which can be measured in the local environment at the site of inflammation, as reliable predictive and/or diagnostic indicators of the development of chronic inflammation.

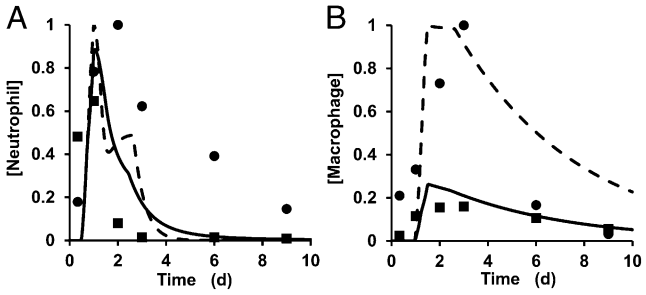

FIGURE 5. Modeling predictions capture experimentally observed chronic inflammatory kinetics. Modeling predictions and experimental validation for acute inflammation, taken from Fig. 3 (■), are shown here for comparison purposes. In Fig. 3A–D, the computational predictions and experimental data were normalized (separately) to the maximum value. (Note that normalization in this figure is different from that for Fig. 3A and 3B, because the maximum values in the data sets were different.) Solid (acute inflammation) and dashed (chronic inflammation) lines show model predictions. ■ show experimental data for acute inflammation; ● show experimental data for chronic inflammation. Chronic inflammation in the computational model was induced by increasing macrophage influx rate (P7) 5-fold from its default value. Chronic inflammation with delayed healing in mice was obtained by a 100-fold higher endotoxin dose given i.p. (16). Shown are the total neutrophil (**A**) and macrophage (**B**) concentrations.

Macrophages are regarded as the most multifunctional immune cells, influencing nearly all phases of the inflammatory response. The possibility of their targeted manipulation has naturally been the subject of extensive investigations (59–61). Because macrophages are the major producers of cytokines with pro- or anti-inflammatory properties (41, 59, 61), any significant disruption in macrophage behavior may be expected to alter the balance of cytokines in the inflammatory milieu. Elevated levels of macrophage infiltration can lead to wound fibrosis (59). At the same time, severe early inhibition of macrophage signaling (as well as macrophage ablation during later stages of inflammation) results in delayed healing in mouse wound models (62, 63), suggesting that initial macrophage availability (and, therefore, their sufficient influx) is necessary for normal inflammatory response. Thus, our modeling prediction regarding macrophage flux modulation as possibly the strongest overall inducer of chronic inflammation can perhaps be readily rationalized. Nevertheless, it is noteworthy that, in our model, macrophage flux rates have a larger impact on cytokine production than any of the cytokines' individual production and degradation rates. This effect might be (at least partially) due to the functional redundancy exhibited by some cytokines, so that a change in the production or degradation rate of one cytokine can be compensated for by the action of the others. For example, TNF-α and MIP-1α act as chemoattractants for macrophages and perform positive regulation of the production of other pro-inflammatory

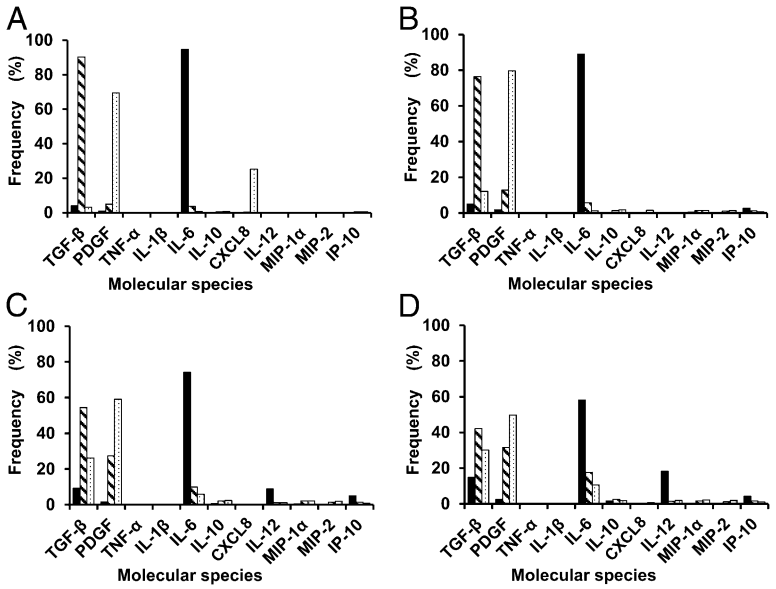

FIGURE 6. Sensitivity analysis identifies IL-6, TGF-β, and PDGF as the most sensitive indicators of chronic inflammation induced by macrophage influx manipulation. Shown are the percentages of the total 10,000 random parameter sets for which different molecular species in the model demonstrated the largest (solid bars), second largest (striped bars), and third largest (stippled bars) relative change induced by modulation of macrophage influx. Model predictions are shown for day 2 (**A**), day 4 (**B**), day 10 (**C**), and day 16 (**D**) after inflammation induction.

cytokines (Supplemental Table I). In contrast, because of a lack of compensatory mechanisms, a disruption in the migration of pro- and/or anti-inflammatory macrophages has a direct and global impact on cytokine production and downstream processes.

A need for guided therapy has been well documented in the treatment of chronic wounds resulting from military trauma (19, 64). A treating clinician's decision to surgically close a wound is commonly based on subjective and somewhat arbitrary measures, such as the patient's general condition, the appearance of bones and soft tissues, and visual signs of infection or necrosis (65), which are poor indicators of the local inflammatory condition (66). This often has led to wound dehiscence and nonhealing wounds. Our work was largely motivated by the need to find molecular indicators that are characteristic of the local wound environment and are less susceptible to systemic influences and, therefore, better reflect ongoing local inflammation.

Our modeling analysis showed that three molecular mediators (IL-6, TGF-β, and PDGF) may be expected to demonstrate consistently large relative changes in their local concentrations induced by independent variations in macrophage influx or efflux rates (Figs. 6, 7). In our analysis, the IL-6 level ranked as the most sensitive indicator of local changes in both macrophage flux parameters. This is consistent with a recent clinical study by Hawksworth et al. (19), who identified IL-6 as an informative indicator of delayed wound healing. However, the comparatively small subject group and limited temporal resolution of this study indicate the need for additional evidence. Our modeling analysis, which involved an extensive parameter randomization, complements these clinical results and suggests that IL-6 may be considered an informative molecular indicator of chronic inflammation for a wide range of scenarios. Furthermore, the model-predicted high sensitivity of TGF-β to macrophage flux modulation correlates with its known diverse and numerous roles in the inflammation process (38, 39, 67–69). Although the clinical study by Hawksworth et al. (19) did not report results for TGF-β and PDGF, our computational findings may provide motivation for experimental and clinical testing of these growth factors as additional diagnostic or predictive indicators of chronic inflammation.

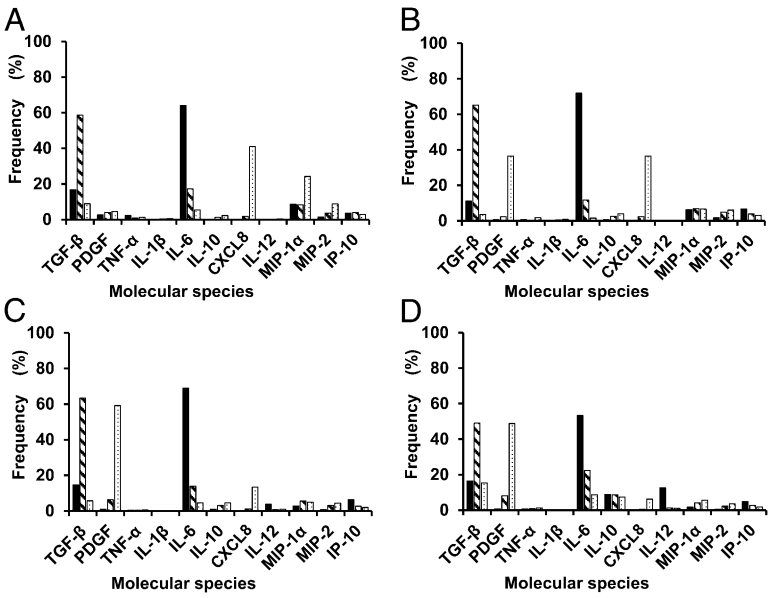

FIGURE 7. Sensitivity analysis identifies IL-6, TGF-β, and PDGF as the most sensitive indicators of chronic inflammation induced by macrophage efflux manipulation. Shown are the percentages of the total 10,000 randomized parameter sets for which different molecular species in the model demonstrated the largest (solid bars), second largest (striped bars), and third largest (stippled bars) relative change induced by modulation of macrophage efflux. Model predictions are shown for day 2 (**A**), day 4 (**B**), day 10 (**C**), and day 16 (**D**) after inflammation induction.

The importance of macrophage flux control elucidated in this study is consistent with the existing view of macrophage dynamics (i.e., monocyte migration, macrophage phenotype conversion, and signaling) as the main driver of effective continuation and resolution of inflammation (61, 70, 71). The migrating blood monocytes are polarized into a wide spectrum of macrophage phenotypes, and the two ends of that spectrum can be characterized as pro-inflammatory macrophage phenotypes (similar to the "classically activated," or M1, phenotype induced in vitro by bacterial LPS and IFN-γ) and anti-inflammatory phenotypes (similar to the "alternatively activated," or M2, phenotype induced in vitro by IL-4 and IL-13), respectively. According to the scenario modeled in this work, M1-type macrophages differentiate into M2-type macrophages, which are responsible for inflammation resolution (59, 60, 70, 71). However, other scenarios of macrophage phenotype progression are conceivable and are supported by existing data. For example, in mouse wounds, distinct circulating monocyte subsets can be recruited to the injury site in a temporally ordered manner and subsequently differentiate into distinct macrophage phenotypes (59). Specifically, the first and second groups of monocytes sequentially entering the wound site give rise to macrophages with phenotypes resembling those for classical and alternative activation, respectively. Interestingly, this scenario is IL-4 and IL-13 independent, as evidenced by the presence of M2-type macrophages in the wounds of IL-4Ra–knockout mice and by the negligible levels of IL-4 and IL-13 at the wound site (59, 72). Furthermore, in some cases, accumulation of substantial numbers of M2-type macrophages is driven primarily by IL-4-dependent proliferation of tissue-resident macrophages, independently of blood monocyte recruitment (73). Such scenarios potentially can be stimulated and modulated in vivo by a myriad of molecular and cellular processes. Indeed, it was suggested that the M1-type to M2-type phenotypic transitions are impacted by various factors, including macrophage interaction with the extracellular matrix, neutrophils, cellular debris, and other soluble molecular mediators, such as IL-10 and TGF-β (59, 60, 74, 75).

In addition to local regulation, systemic influences, including immune complexes, PGs, and glucocorticoids, may determine the phenotypic fate of the monocytes migrating to the inflammation site. For example, macrophages differentiated in the presence of the glucocorticoid dexamethasone exhibit increased sensitivity to TGF-β resulting from an increase in TGF-β receptor expression and induced lipid uptake (76). However, the relative contributions of these numerous factors to macrophage polarization, as well as the complex and synergistic interactions between the factors, are unknown.

The choice of driver for the macrophage phenotypic transition for our model (i.e., pro-inflammatory macrophage phagocytosis of apoptotic neutrophils) was based on the availability of experimental data that could be translated into a modeling framework. Indeed, this mechanism, which is supported by experimental evidence (40–42, 59, 75), robustly drove the macrophage phenotypic transitions in our simulations. Although IL-4 and IL-13 might further modulate this mechanism, their primary contribution in vivo appears to be the connection between innate and adaptive immune systems, because their sustained production is predominantly due to adaptive immune system cells (74). However, because of our emphasis on the self-modulating function of innate immunity and the limitations in our understanding of the interactions between innate and adaptive immunity, we do not model that connection in this study. The possible contributions of other molecular mediators to the functional effects of macrophage polarization were partially reflected through the IL-10– and TGF-β–mediated reduction in pro-inflammatory cytokine production rates. Although our approach to modeling macrophage phenotype conversion is, by necessity, an oversimplification of the molecular and cellular events shaping the transition to the inflammation-resolution phase, it may provide a reference point for future studies specifically focused on macrophage-polarization mechanisms.

The main limitations of this study arise from the simplifications needed to develop a mathematical description of the incredibly complex cellular and molecular interactions that occur during normal and pathological inflammation. First, our model focuses on general aspects of inflammation and does not reflect the specifics of certain inflammation scenarios, such as burns or bacterial infection. Moreover, we do not explicitly define tissue-specific cells, such as resident macrophages, mast cells, and connective tissue cells. Our model is based on the notion that key participants (neutrophils and macrophages) and interactions in the local inflammatory process may be sufficiently similar across many, or most, inflammatory situations (3, 11, 14, 16, 52, 57, 77, 78). Therefore, although we modeled chronic inflammation in (traumatic) wounds, we expect that our findings may be applicable in other contexts, which is supported by comparisons of our modeling results with experimental studies of noninjury-induced inflammation (Figs. 3, 5). Second, our main goal was to develop a computational model relevant for human inflammation, yet our model training and validation were performed using data for rat and mouse (in addition to human) experimental models. Although interspecies differences in the details of the inflammatory response may occur, the use of animal models is a mainstay of immunity research (79). As a result, several experimental datasets that were indispensable for our modeling efforts had been obtained with animal models, whereas analogous datasets for human experimental models were not available. Third, in most cases, we assume constant (but cell phenotype dependent) cytokine production and cell activation rates and do not explicitly consider intracellular signaling pathways that regulate such production and activation. We chose this approach because separation of intra- and intercellular kinetic scales could sharpen our focus on cell phenotype dynamics and general molecular mediator–production patterns, which aligned with the main goals of this work. Fourth, in the model, we reduced the variety of macrophage phenotypes that are known to exist at inflammatory sites to only two, which gave us the benefit of modeling tractability. Finally, our model represents pro-inflammatory macrophage phenotype conversion as the only source of anti-inflammatory macrophages, whereas independently activated, "second-wave" migration of anti-inflammatory macrophages into the inflammation site is a plausible alternative (60, 71). Further studies are needed to develop and validate more detailed representations of the inflammatory process and its perturbations.

Because of the recognition of the role of chronic inflammation in different pathologies, the need for efficient therapies and early diagnostic molecular tools for chronic inflammation has rapidly increased. Our modeling suggests that narrowly targeting one single mechanism may not always be an efficacious strategy to treat chronic inflammation, because it can be triggered and maintained by different mechanistic factors at different time points (Fig. 4). This might explain the limited efficacy of some currently used therapeutic interventions, such as nonsteroidal anti-inflammatory drugs, which target the production of PGs (80). Likewise, targeted neutralization of a single pro-inflammatory cytokine, such as IL-1β or TNF-α, used to treat chronic inflammatory pathologies associated with cancer (81), rheumatoid arthritis (82), infection (83), and impaired cutaneous wounds (84, 85), has seen limited success. Rigorous experimental testing and extensive clinical evaluation

of our computational modeling results might contribute to the development of timely therapies for chronic inflammation and provide a panel of informative molecular indicators for objective clinical assessment of inflammatory scenarios in injury or disease.

Software availability

The MATLAB code for our computational analyses is freely available and can be downloaded from the *Journal of Immunology* Web site.

Acknowledgments

We thank the three anonymous reviewers whose comments helped to improve the article.

Disclosures

The authors have no financial conflicts of interest.

References

1. Medzhitov, R. 2008. Origin and physiological roles of inflammation. *Nature* 454: 428–435.
2. Nathan, C. 2002. Points of control in inflammation. *Nature* 420: 846–852.
3. Melnicoff, M. J., P. K. Horan, and P. S. Morahan. 1989. Kinetics of changes in peritoneal cell populations following acute inflammation. *Cell. Immunol.* 118: 178–191.
4. Wu, Q., Y. Feng, Y. Yang, W. Jingliu, W. Zhou, P. He, R. Zhou, X. Li, and J. Zou. 2004. Kinetics of the phenotype and function of murine peritoneal macrophages following acute inflammation. *Cell. Mol. Immunol.* 1: 57–62.
5. Kumar, R., G. Clermont, Y. Vodovotz, and C. C. Chow. 2004. The dynamics of acute inflammation. *J. Theor. Biol.* 230: 145–155.
6. Feghali, C. A., and T. M. Wright. 1997. Cytokines in acute and chronic inflammation. *Front. Biosci.* 2: d12–d26.
7. Dinarello, C. A. 2000. Proinflammatory cytokines. *Chest* 118: 503–508.
8. Opal, S. M., and V. A. DePalo. 2000. Anti-inflammatory cytokines. *Chest* 117: 1162–1172.
9. Loots, M. A., E. N. Lamme, J. Zeegelaar, J. R. Mekkes, J. D. Bos, and E. Middelkoop. 1998. Differences in cellular infiltrate and extracellular matrix of chronic diabetic and venous ulcers versus acute wounds. *J. Invest. Dermatol.* 111: 850–857.
10. Nathan, C., and A. Ding. 2010. Nonresolving inflammation. *Cell* 140: 871–882.
11. Hunter, P. 2012. The inflammation theory of disease. The growing realization that chronic inflammation is crucial in many diseases opens new avenues for treatment. *EMBO Rep.* 13: 968–970.
12. Khanna, S., S. Biswas, Y. Shang, E. Collard, A. Azad, C. Kauh, V. Bhasker, G. M. Gordillo, C. K. Sen, and S. Roy. 2010. Macrophage dysfunction impairs resolution of inflammation in the wounds of diabetic mice. *PLoS ONE* 5: e9539.
13. Roy, S., S. Biswas, S. Khanna, G. Gordillo, V. Bergdall, J. Green, C. B. Marsh, L. J. Gould, and C. K. Sen. 2009. Characterization of a preclinical model of chronic ischemic wound. *Physiol. Genomics* 37: 211–224.
14. Navarro-Xavier, R. A., J. Newson, V. L. Silveira, S. N. Farrow, D. W. Gilroy, and J. Bystrom. 2010. A new strategy for the identification of novel molecules with targeted proresolution of inflammation properties. *J. Immunol.* 184: 1516–1525.
15. Zhou, L. J., R. Matsui, and I. Ono. 2000. Development of a chronic skin defect model and a study of cytokine secretion using the model. *Wound Repair Regen.* 8: 304–318.
16. Bystrom, J., I. Evans, J. Newson, M. Stables, I. Toor, N. van Rooijen, M. Crawford, P. Colville-Nash, S. Farrow, and D. W. Gilroy. 2008. Resolution-phase macrophages possess a unique inflammatory phenotype that is controlled by cAMP. *Blood* 112: 4117–4127.
17. Wiegand, C., U. Schönfelder, M. Abel, P. Ruth, M. Kaatz, and U. C. Hipler. 2010. Protease and pro-inflammatory cytokine concentrations are elevated in chronic compared to acute wounds and can be modulated by collagen type I in vitro. *Arch. Dermatol. Res.* 302: 419–428.
18. Gohel, M. S., R. A. Windhaber, J. F. Tarlton, M. R. Whyman, and K. R. Poskitt. 2008. The relationship between cytokine concentrations and wound healing in chronic venous ulceration. *J. Vasc. Surg.* 48: 1272–1277.
19. Hawksworth, J. S., A. Stojadinovic, F. A. Gage, D. K. Tadaki, P. W. Perdue, J. Forsberg, T. A. Davis, J. R. Dunne, J. W. Denobile, T. S. Brown, and E. A. Elster. 2009. Inflammatory biomarkers in combat wound healing. *Ann. Surg.* 250: 1002–1007.
20. Trengove, N. J., H. Bielefeldt-Ohmann, and M. C. Stacey. 2000. Mitogenic activity and cytokine levels in non-healing and healing chronic leg ulcers. *Wound Repair Regen.* 8: 13–25.
21. Trengove, N. J., M. C. Stacey, S. MacAuley, N. Bennett, J. Gibson, F. Burslem, G. Murphy, and G. Schultz. 1999. Analysis of the acute and chronic wound environments: the role of proteases and their inhibitors. *Wound Repair Regen.* 7: 442–452.
22. Utz, E. R., E. A. Elster, D. K. Tadaki, F. Gage, P. W. Perdue, J. A. Forsberg, A. Stojadinovic, J. S. Hawksworth, and T. S. Brown. 2010. Metalloproteinase expression is associated with traumatic wound failure. *J. Surg. Res.* 159: 633–639.
23. Jin, Y. F., H. C. Han, J. Berger, Q. Dai, and M. L. Lindsey. 2011. Combining experimental and mathematical modeling to reveal mechanisms of macrophage-dependent left ventricular remodeling. *BMC Syst. Biol.* 5: 60.
24. Li, N. Y., K. Verdolini, G. Clermont, Q. Mi, E. N. Rubinstein, P. A. Hebda, and Y. Vodovotz. 2008. A patient-specific in silico model of inflammation and healing tested in acute vocal fold injury. *PLoS ONE* 3: e2789.
25. Menke, N. B., J. W. Cain, A. Reynolds, D. M. Chan, R. A. Segal, T. M. Witten, D. G. Bonchev, R. F. Diegelmann, and K. R. Ward; Virginia Commonwealth University Reanimation, Engineering Shock Center, The Wound Healing Group. 2010. An in silico approach to the analysis of acute wound healing. *Wound Repair Regen.* 18: 105–113.
26. Mi, Q., B. Rivière, G. Clermont, D. L. Steed, and Y. Vodovotz. 2007. Agent-based model of inflammation and wound healing: insights into diabetic foot ulcer pathology and the role of transforming growth factor-beta1. *Wound Repair Regen.* 15: 671–682.
27. Nieman, G., D. Brown, J. Sarkar, B. Kubiak, C. Ziraldo, J. Dutta-Moscato, C. Vieau, D. Barclay, L. Gatto, K. Maier, et al. 2012. A two-compartment mathematical model of endotoxin-induced inflammatory and physiologic alterations in swine. *Crit. Care Med.* 40: 1052–1063.
28. Prince, J. M., R. M. Levy, J. Bartels, A. Baratt, J. M. Kane, III, C. Lagoa, J. Rubin, J. Day, J. Wei, M. P. Fink, et al. 2006. In silico and in vivo approach to elucidate the inflammatory complexity of CD14-deficient mice. *Mol. Med.* 12: 88–96.
29. Reynolds, A., J. Rubin, G. Clermont, J. Day, Y. Vodovotz, and G. Bard Ermentrout. 2006. A reduced mathematical model of the acute inflammatory response: I. Derivation of model and analysis of anti-inflammation. *J. Theor. Biol.* 242: 220–236.
30. Torres, A., T. Bentley, J. Bartels, J. Sarkar, D. Barclay, R. Namas, G. Constantine, R. Zamora, J. C. Puyana, and Y. Vodovotz. 2009. Mathematical modeling of posthemorrhage inflammation in mice: studies using a novel, computer-controlled, closed-loop hemorrhage apparatus. *Shock* 32: 172–178.
31. Waugh, H. V., and J. A. Sherratt. 2006. Macrophage dynamics in diabetic wound dealing. *Bull. Math. Biol.* 68: 197–207.
32. Waugh, H. V., and J. A. Sherratt. 2007. Modeling the effects of treating diabetic wounds with engineered skin substitutes. *Wound Repair Regen.* 15: 556–565.
33. Smith, A. M., J. A. McCullers, and F. R. Adler. 2011. Mathematical model of a three-stage innate immune response to a pneumococcal lung infection. *J. Theor. Biol.* 276: 106–116.
34. Pierce, G. F., T. A. Mustoe, J. Lingelbach, V. R. Masakowski, G. L. Griffin, R. M. Senior, and T. F. Deuel. 1989. Platelet-derived growth factor and transforming growth factor-beta enhance tissue repair activities by unique mechanisms. *J. Cell Biol.* 109: 429–440.
35. Pai, R., H. Ha, M. A. Kirschenbaum, and V. S. Kamanna. 1996. Role of tumor necrosis factor-alpha on mesangial cell MCP-1 expression and monocyte migration: mechanisms mediated by signal transduction. *J. Am. Soc. Nephrol.* 7: 914–923.
36. Wang, J. M., B. Sherry, M. J. Fivash, D. J. Kelvin, and J. J. Oppenheim. 1993. Human recombinant macrophage inflammatory protein-1 alpha and -beta and monocyte chemotactic and activating factor utilize common and unique receptors on human monocytes. *J. Immunol.* 150: 3022–3029.
37. Deuel, T. F., R. M. Senior, J. S. Huang, and G. L. Griffin. 1982. Chemotaxis of monocytes and neutrophils to platelet-derived growth factor. *J. Clin. Invest.* 69: 1046–1049.
38. Wahl, S. M., D. A. Hunt, L. M. Wakefield, N. McCartney-Francis, L. M. Wahl, A. B. Roberts, and M. B. Sporn. 1987. Transforming growth factor type β induces monocyte chemotaxis and growth factor production. *Proc. Natl. Acad. Sci. USA* 84: 5788–5792.
39. Brandes, M. E., U. E. Mai, K. Ohura, and S. M. Wahl. 1991. Type I transforming growth factor-beta receptors on neutrophils mediate chemotaxis to transforming growth factor-beta. *J. Immunol.* 147: 1600–1606.
40. Byrne, A., and D. J. Reen. 2002. Lipopolysaccharide induces rapid production of IL-10 by monocytes in the presence of apoptotic neutrophils. *J. Immunol.* 168: 1968–1977.
41. Fadok, V. A., D. L. Bratton, A. Konowal, P. W. Freed, J. Y. Westcott, and P. M. Henson. 1998. Macrophages that have ingested apoptotic cells in vitro inhibit proinflammatory cytokine production through autocrine/paracrine mechanisms involving TGF-beta, PGE2, and PAF. *J. Clin. Invest.* 101: 890–898.
42. Arnold, L., A. Henry, F. Poron, Y. Baba-Amer, N. van Rooijen, A. Plonquet, R. K. Gherardi, and B. Chazaud. 2007. Inflammatory monocytes recruited after skeletal muscle injury switch into antiinflammatory macrophages to support myogenesis. *J. Exp. Med.* 204: 1057–1069.
43. Grainger, D. J., L. Wakefield, H. W. Bethell, R. W. Farndale, and J. C. Metcalfe. 1995. Release and activation of platelet latent TGF-beta in blood clots during dissolution with plasmin. *Nat. Med.* 1: 932–937.
44. Harpel, J. G., C. N. Metz, S. Kojima, and D. B. Rifkin. 1992. Control of transforming growth factor-beta activity: latency vs. activation. *Prog. Growth Factor Res.* 4: 321–335.
45. Andrei, C., C. Dazzi, L. Lotti, M. R. Torrisi, G. Chimini, and A. Rubartelli. 1999. The secretory route of the leaderless protein interleukin 1beta involves exocytosis of endolysosome-related vesicles. *Mol. Biol. Cell* 10: 1463–1475.
46. Hazuda, D. J., J. C. Lee, and P. R. Young. 1988. The kinetics of interleukin 1 secretion from activated monocytes. Differences between interleukin 1 alpha and interleukin 1 beta. *J. Biol. Chem.* 263: 8473–8479.
47. Newman, S. L., J. E. Henson, and P. M. Henson. 1982. Phagocytosis of senescent neutrophils by human monocyte-derived macrophages and rabbit inflammatory macrophages. *J. Exp. Med.* 156: 430–442.

48. Hart, S. P., K. M. Alexander, and I. Dransfield. 2004. Immune complexes bind preferentially to Fc gamma RIIA (CD32) on apoptotic neutrophils, leading to augmented phagocytosis by macrophages and release of proinflammatory cytokines. *J. Immunol.* 172: 1882–1887.
49. Ren, Y., Y. Xie, G. Jiang, J. Fan, J. Yeung, W. Li, P. K. Tam, and J. Savill. 2008. Apoptotic cells protect mice against lipopolysaccharide-induced shock. *J. Immunol.* 180: 4978–4985.
50. Mitrophanov, A. Y., G. Churchward, and M. Borodovsky. 2007. Control of *Streptococcus pyogenes* virulence: modeling of the CovR/S signal transduction system. *J. Theor. Biol.* 246: 113–128.
51. Wei, H., M. A. Nearing, and J. J. Stone. 2007. A comprehensive sensitivity analysis framework for model evaluation and improvement using a case study of the rangeland hydrology and erosion model. *Trans. ASABE* 50: 945–953.
52. Engelhardt, E., A. Toksoy, M. Goebeler, S. Debus, E. B. Bröcker, and R. Gillitzer. 1998. Chemokines IL-8, GROalpha, MCP-1, IP-10, and Mig are sequentially and differentially expressed during phase-specific infiltration of leukocyte subsets in human wound healing. *Am. J. Pathol.* 153: 1849–1860.
53. Yang, L., C. X. Qiu, A. Ludlow, M. W. Ferguson, and G. Brunner. 1999. Active transforming growth factor-β in wound repair: determination using a new assay. *Am. J. Pathol.* 154: 105–111.
54. Kum, W. W., S. B. Cameron, R. W. Hung, S. Kalyan, and A. W. Chow. 2001. Temporal sequence and kinetics of proinflammatory and anti-inflammatory cytokine secretion induced by toxic shock syndrome toxin 1 in human peripheral blood mononuclear cells. *Infect. Immun.* 69: 7544–7549.
55. Cao, C., D. A. Lawrence, D. K. Strickland, and L. Zhang. 2005. A specific role of integrin Mac-1 in accelerated macrophage efflux to the lymphatics. *Blood* 106: 3234–3241.
56. Sisco, M., J. D. Chao, I. Kim, J. E. Mogford, T. N. Mayadas, and T. A. Mustoe. 2007. Delayed wound healing in Mac-1-deficient mice is associated with normal monocyte recruitment. *Wound Repair Regen.* 15: 566–571.
57. Fillion, I., N. Ouellet, M. Simard, Y. Bergeron, S. Sato, and M. G. Bergeron. 2001. Role of chemokines and formyl peptides in pneumococcal pneumonia-induced monocyte/macrophage recruitment. *J. Immunol.* 166: 7353–7361.
58. Mori, R., T. Kondo, T. Ohshima, Y. Ishida, and N. Mukaida. 2002. Accelerated wound healing in tumor necrosis factor receptor p55-deficient mice with reduced leukocyte infiltration. *FASEB J.* 16: 963–974.
59. Brancato, S. K., and J. E. Albina. 2011. Wound macrophages as key regulators of repair: origin, phenotype, and function. *Am. J. Pathol.* 178: 19–25.
60. Gordon, S., and P. R. Taylor. 2005. Monocyte and macrophage heterogeneity. *Nat. Rev. Immunol.* 5: 953–964.
61. Koh, T. J., and L. A. DiPietro. 2011. Inflammation and wound healing: the role of the macrophage. *Expert Rev. Mol. Med.* 13: e23.
62. Mirza, R., L. A. DiPietro, and T. J. Koh. 2009. Selective and specific macrophage ablation is detrimental to wound healing in mice. *Am. J. Pathol.* 175: 2454–2462.
63. Lucas, T., A. Waisman, R. Ranjan, J. Roes, T. Krieg, W. Müller, A. Roers, and S. A. Eming. 2010. Differential roles of macrophages in diverse phases of skin repair. *J. Immunol.* 184: 3964–3977.
64. Hahm, G., J. J. Glaser, and E. A. Elster. 2011. Biomarkers to predict wound healing: the future of complex war wound management. *Plast. Reconstr. Surg.* 127(Suppl. 1): 21S–26S.
65. Crane, N. J., T. S. Brown, K. N. Evans, J. S. Hawksworth, S. Hussey, D. K. Tadaki, and E. A. Elster. 2010. Monitoring the healing of combat wounds using Raman spectroscopic mapping. *Wound Repair Regen.* 18: 409–416.
66. Forsberg, J. A., E. A. Elster, R. C. Andersen, E. Nylen, T. S. Brown, M. W. Rose, A. Stojadinovic, K. L. Becker, and F. X. McGuigan. 2008. Correlation of procalcitonin and cytokine expression with dehiscence of wartime extremity wounds. *J. Bone Joint Surg. Am.* 90: 580–588.
67. Chantry, D., M. Turner, E. Abney, and M. Feldmann. 1989. Modulation of cytokine production by transforming growth factor-beta. *J. Immunol.* 142: 4295–4300.
68. Maeda, H., H. Kuwahara, Y. Ichimura, M. Ohtsuki, S. Kurakata, and A. Shiraishi. 1995. TGF-beta enhances macrophage ability to produce IL-10 in normal and tumor-bearing mice. *J. Immunol.* 155: 4926–4932.
69. Tsunawaki, S., M. Sporn, A. Ding, and C. Nathan. 1988. Deactivation of macrophages by transforming growth factor-beta. *Nature* 334: 260–262.
70. Murray, P. J., and T. A. Wynn. 2011. Protective and pathogenic functions of macrophage subsets. *Nat. Rev. Immunol.* 11: 723–737.
71. Lawrence, T., and G. Natoli. 2011. Transcriptional regulation of macrophage polarization: enabling diversity with identity. *Nat. Rev. Immunol.* 11: 750–761.
72. Daley, J. M., S. K. Brancato, A. A. Thomay, J. S. Reichner, and J. E. Albina. 2010. The phenotype of murine wound macrophages. *J. Leukoc. Biol.* 87: 59–67.
73. Jenkins, S. J., D. Ruckerl, P. C. Cook, L. H. Jones, F. D. Finkelman, N. van Rooijen, A. S. MacDonald, and J. E. Allen. 2011. Local macrophage proliferation, rather than recruitment from the blood, is a signature of TH2 inflammation. *Science* 332: 1284–1288.
74. Mosser, D. M., and J. P. Edwards. 2008. Exploring the full spectrum of macrophage activation. *Nat. Rev. Immunol.* 8: 958–969.
75. Fox, S., A. E. Leitch, R. Duffin, C. Haslett, and A. G. Rossi. 2010. Neutrophil apoptosis: relevance to the innate immune response and inflammatory disease. *J. Innate Immun.* 2: 216–227.
76. Gratchev, A., J. Kzhyshkowska, S. Kannookadan, M. Ochsenreiter, A. Popova, X. Yu, S. Mamidi, E. Stonehouse-Usselmann, I. Muller-Molinet, L. Gooi, and S. Goerdt. 2008. Activation of a TGF-beta-specific multistep gene expression program in mature macrophages requires glucocorticoid-mediated surface expression of TGF-beta receptor II. *J. Immunol.* 180: 6553–6565.
77. Oh, S. F., M. Dona, G. Fredman, S. Krishnamoorthy, D. Irimia, and C. N. Serhan. 2012. Resolvin E2 formation and impact in inflammation resolution. *J. Immunol.* 188: 4527–4534.
78. Ashley, N. T., Z. M. Weil, and R. J. Nelson. 2012. Inflammation: mechanisms, costs, and natural variation. *Annu. Rev. Ecol. Evol. Syst.* 43: 385–406.
79. Bryant, C. E., and T. P. Monie. 2012. Mice, men and the relatives: cross-species studies underpin innate immunity. *Open Biol.* 2: 120015.
80. Vane, J. R., and R. M. Botting. 1998. Mechanism of action of nonsteroidal anti-inflammatory drugs. *Am. J. Med.* 104 (Suppl. 1): 2S–8S; discussion 21S–22S.
81. Lewis, A. M., S. Varghese, H. Xu, and H. R. Alexander. 2006. Interleukin-1 and cancer progression: the emerging role of interleukin-1 receptor antagonist as a novel therapeutic agent in cancer treatment. *J. Transl. Med.* 4: 48.
82. Feldmann, M., and R. N. Maini. 2001. Anti-TNF alpha therapy of rheumatoid arthritis: what have we learned? *Annu. Rev. Immunol.* 19: 163–196.
83. Teti, G., G. Mancuso, and F. Tomasello. 1993. Cytokine appearance and effects of anti-tumor necrosis factor alpha antibodies in a neonatal rat model of group B streptococcal infection. *Infect. Immun.* 61: 227–235.
84. Ashcroft, G. S., M. J. Jeong, J. J. Ashworth, M. Hardman, W. Jin, N. Moutsopoulos, T. Wild, N. McCartney-Francis, D. Sim, G. McGrady, et al. 2012. Tumor necrosis factor-alpha (TNF-α) is a therapeutic target for impaired cutaneous wound healing. *Wound Repair Regen.* 20: 38–49.
85. Thomay, A. A., J. M. Daley, E. Sabo, P. J. Worth, L. J. Shelton, M. W. Harty, J. S. Reichner, and J. E. Albina. 2009. Disruption of interleukin-1 signaling improves the quality of wound healing. *Am. J. Pathol.* 174: 2129–2136.
86. Wakefield, L. M., D. M. Smith, K. C. Flanders, and M. B. Sporn. 1988. Latent transforming growth factor-beta from human platelets. A high molecular weight complex containing precursor sequences. *J. Biol. Chem.* 263: 7646–7654.
87. Werner, S., and R. Grose. 2003. Regulation of wound healing by growth factors and cytokines. *Physiol. Rev.* 83: 835–870.
88. Bellingan, G. J., P. Xu, H. Cooksley, H. Cauldwell, A. Shock, S. Bottoms, C. Haslett, S. E. Mutsaers, and G. J. Laurent. 2002. Adhesion molecule-dependent mechanisms regulate the rate of macrophage clearance during the resolution of peritoneal inflammation. *J. Exp. Med.* 196: 1515–1521.